Phys. Status Solidi A **210**, No. 8, 1606–1611 (2013) / **DOI** 10.1002/pssa.201228477

physica status solidi a
www.pss-a.com
applications and materials science

Hydrogen influence on the electrical properties of sputtered InN thin films

Marina Sparvoli[*,1], **Ronaldo D. Mansano**[1], **and José F. D. Chubaci**[**,2]

[1] Departamento de Engenharia Elétrica, Escola Politécnica da Universidade de São Paulo, São Paulo 05508-900, Brazil
[2] Instituto de Física da Universidade de São Paulo, São Paulo 05314-970, Brazil

Received 12 July 2012, revised 19 February 2013, accepted 14 March 2013
Published online 22 April 2013

Keywords electrical properties, InN, sputtering, III–V semiconductors, thin films

* Corresponding author: e-mail marinsparvoli@yahoo.com.br, Phone: +55 11 8533 3394, Fax: +55 11 3091 5664
** e-mail chubaci@if.usp.br, Phone: +55 11 3091 6684, Fax: +55 11 3031 2742

The narrow indium nitride (InN) bandgap has generated great interest for applications such as high-efficiency solar cells, light-emitting diodes, laser diodes, and high-frequency transistors. The ability to fabricate both p-type and n-type InN is essential for the production of these devices; however, InN is naturally an n-type semiconductor. This work's main objective is to study the influence of the deposition process using nitrogen and hydrogen on the optical and electrical properties of RF reactive sputtered InN films. During deposition, a hydrogen percentage is incorporated with the InN and the hydrogen works like a source of acceptors. Hydrogen incorporation becomes interesting as these materials are developed for photovoltaic and optoelectronic application. Fourier transform infrared spectra showed the presence of In–N bonding and In–H bonding.

1 Introduction Indium nitride thin films are naturally n-type. This does not mean that during the growth process other elements could not be introduced to decrease the density of negative carriers or even to change the character to p-type semiconductor.

The electrical properties of a device depend directly on the nature and configuration of its composing materials. For example, the junction between n-type (electron conductors) and p-type (hole conductors) materials while forming a diode junction can form n–p–n or p–n–p transistors. The ability to produce both p-type and n-type InN opens up a range of possibilities to produce highly efficient devices such as solar cells, extremely sensitive sensors, laser diodes and LEDs [1].

It is common to get n-type indium nitride; even without doping InN is n-type. But it is almost impossible to produce the p-type material. Walukiewicz, in his research, showed that the peculiar electronic structure of InN requires an abnormally large amount of energy to remove electrons from its conduction band and make way for the holes.

The indium nitride crystals are riddled with defects, reaching tens of billions per square centimetre. Large quantities of atoms in these defects are unable to form bonds with their neighbors and as the energy level of these defects is located exactly in the middle of the forbidden band of InN these dangling bonds are unable to donate spare electrons to the conduction band. Besides, the oxygen and metallic indium present in InN films promote the n-type InN orientation [2]. The surface of InN is by definition an n-type and conductive semiconductor [3].

This work's main objective is to study the influence of deposition process on the optical and electrical properties of RF reactive-sputtered InN films using nitrogen and hydrogen. Hydrogen works like a source of acceptors in InN films and eliminates oxygen. It can bind to the native defects and other impurities that are present in the host matrix and change their electrical characteristics [4].

2 Experimental In this work, silicon wafers with resistivity in the range of 10–20 Ω cm, 3-in. diameter, 0.28-mm thick, p-type, (100) were used. High-purity N_2 and H_2 gas (99.999%) and an In target were used in the deposition process (Table 1).

Initially, a cleaning process ($4H_2SO_4 + 1H_2O_2$) followed by HF dipping (2%), was performed. After the cleaning process, the deposition of InN films was performed in a magnetron sputtering system using a pure In target, nitrogen and hydrogen as process gases and 200 W constant RF power. Four hydrogen gas concentrations were used in the deposition processes (0, 2, 4, and 8%). Table 2 shows the deposited films parameters.

Table 1 Deposition parameters.

target	99.999% indium, 4 in. diameter
substrate	silicon p-type
substrate distance	6 cm
base pressure	5 mTorr
RF power	200 W
H_2 gas concentrations	0, 2, 4, and 8%
gas flow	30 sccm

Table 2 Deposited indium nitride thin film thickness and growth rate.

sample	thickness (nm)	growth rate (nm min^{-1})
0% H_2	938	15.63
2% H_2	691	11.51
4% H_2	688	13.61
8% H_2	877	14.62

The electrical properties of the films (resistivity, mobility, and carrier concentration) were determined by Hall-effect measurements using silver contacts by the van der Pauw technique.

The Fourier transform infrared (FTIR) technique was used to study the bonding structures of the films. The FTIR study of the indium nitride was performed to gain more information about composition and structure of the material and to characterize the bond types. This analysis was performed in absorbance mode with a resolution of 4 cm^{-1} in the 2500–400 cm^{-1} wave number range.

To obtain the bandgap, Tauc analysis was used. This is a method based in UV–vis reflectance spectra. Reflectance measurements were performed with a near-infrared–visible–UV spectrometer (scanning spectral range between 250 and 2500 nm). Emission from a halogen light source was used to provide the spectral range for the measurements in samples. The reflected light from the UV to near-infrared spectral region was collected using different detectors.

The XRD patterns of the InN films deposited on silicon substrate at room temperature for various hydrogen gas concentrations were measured. X-ray diffraction is a powerful, noncontact method used in order to understand the crystalline phases in bulk materials, thin films, and powder samples. The principle of this technique involves X-ray waves interacting with atomic planes in materials that will exhibit the phenomenon of diffraction [5].

Rutherford backscattering spectrometry (RBS) was used to estimate the stoichiometry of the films. The percenteage of each element, oxygen, nitrogen, and indium was determined by the SIMNRA program.

3 Results It is demonstrated that hydrogen acts as a source of electrons for InN when these thin films are deposited by processes without a plasma. Van de Walle et al. predicted a different influence of hydrogen in InN than in other nitrides. Hydrogen is primarily thought of as an interstitial impurity. In most semiconductors such as GaN or AlN, interstitial hydrogen is amphoteric: it is stable as a donor in p-type and as an acceptor in n-type material, always counteracting the prevailing conductivity. However, interstitial hydrogen acts exclusively as a donor in indium nitride and can cause a breaking of an N–In chemical bond. In their work, Van de Walle et al. showed that in addition to occurring on interstitial sites, hydrogen can substitute for nitrogen. Substitutional hydrogen has a lower formation energy than nitrogen vacancy; it is stable and acts as a double donor in InN [2, 6–10].

In the sputtering case, there exists the possibility that the mechanism may be different. Because this process enables the deposition of thin films of InN in an environment of a plasma, the hydrogen is ionized. This gas offers an increase of holes in the material when the hydrogen is bonded with an indium atom itself (“kidnapping” an InN electron) during the deposition process, producing InH and making the film a p-type semiconductor [11, 12].

The results obtained by the Hall effect measurements show that, in general, the resistivity of the films deposited on Si is very low. This can be associated with a high leakage current. The resistivity of the pure InN and hydrogenated InN was in the range 2.18–61.9 mΩ cm, which are many orders of magnitude lower than typical semiconductors. The low resistivity indicates a high density of charge carriers. These results are very similar to most of the thin films studied by previous workers; for example, Goldys and coworkers [6] reported values within the range 1.6–4 mΩ cm. These low resistivities are caused by impurities in the samples. In Table 3, it can be observed that samples deposited with

Table 3 Electrical measurements results of the films.

sample	mobility (cm^2/V s)	density (cm^{-3})	resistivity four-point (mΩ cm)	resistivity Hall effect (mΩ cm)	type four-point	type Hall effect
0% H_2	0.19	1.94×10^{21}	4.18	4.70	n	n
2% H_2	29.97	8.26×10^{18}	55.20	61.90	p	p
4% H_2	3.10	3.61×10^{20}	2.48	2.18	p	p
8% H_2	4.47	1.73×10^{20}	7.34	6.11	p	p

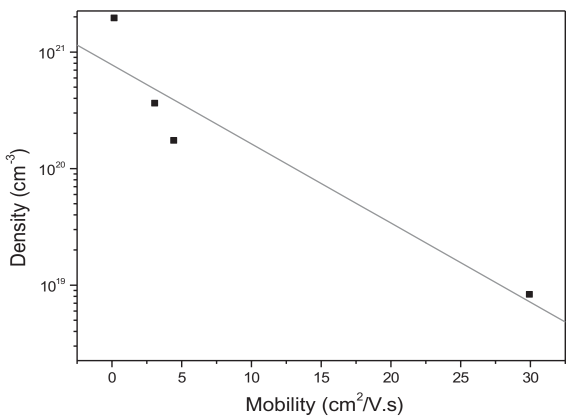

Figure 1 Electrical measurement results of the films: density versus mobility.

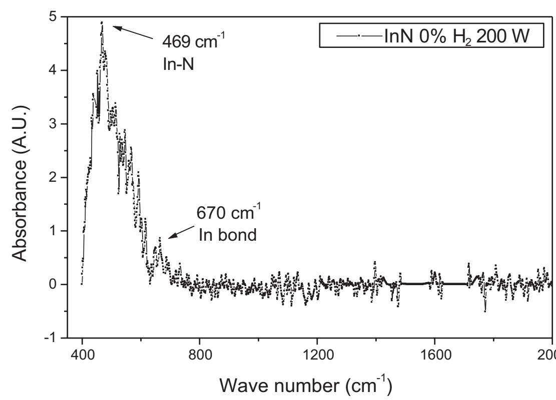

Figure 2 FT-IR peaks of the films produced without hydrogen.

hydrogen are p-type semiconductors. This was proven by Hall effect and four-point measurements.

The mobility is low if compared with other semiconductors. The density decreases exponentially as a function of this parameter (Fig. 1).

It is observed in Table 4 that there is a prominent peak in the region between 466 and 478 cm^{-1} that occurs for all InN samples (Figs. 2–5). This peak corresponds to the In–N single bond. The second peak occurs at 672–678 cm^{-1} and belongs to metallic indium. The third peak corresponds to the double bond In = N at 1156 cm^{-1}. The fourth peak corresponds to the In–H single bond (1657–1677 cm^{-1}) and it proves that the hydrogen was incorporated in the thin film.

It is shown that the hydrogen incorporation eliminates the metallic indium. Although the binding energy or enthalpy of indium hydride (243.1 kJ mol^{-1}) and indium nitride (282.2 kJ mol^{-1}) are lower than the indium oxide enthalpy (320.1 kJ mol^{-1}), the low temperature (90 °C) of the deposition process by sputtering and the hydrogen presence in the chamber allowed the formation of In–H bonds in an indium nitride matrix. The hydrogen used as process gas promotes the oxygen elimination from the deposition ambient.

RBS measurements confirm oxygen elimination in the samples (Table 5 and Figs. 6–8).

RBS was used to estimate the stoichiometry. The relative quantities obtained from RBS spectra analysis in pure InN

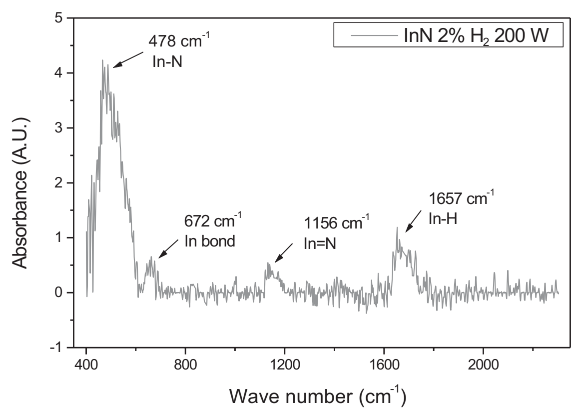

Figure 3 FT-IR peaks of the films produced with 2% hydrogen.

sample are 8% O, 65% N, and 27% In due to contamination by oxygen in the deposition process (Figs. 9–12).

Metallic indium elimination can be verified through analysis by the XRD technique.

Table 6 shows the XRD peaks of the InN thin films grown on glass substrates at room temperature. It is seen that all the InN samples show an intense and thin diffraction peak at around 31°, which is assigned to the (0002) diffraction of InN with a wurtzite structure [13, 14]. The bulk InN 0002

Table 4 FT-IR peaks of the films produced without hydrogen in the gas mixture and with 2, 4, and 8% of hydrogen.

sample	peak 1 position	abs.	peak 2 position	abs.	peak 3 position	abs.	peak 4 position	abs.
0% H_2	469 cm^{-1}	4.88	670 cm^{-1}	0.80	–	–	–	–
2% H_2	478 cm^{-1}	4.10	672 cm^{-1}	0.57	1156 cm^{-1}	0.51	1657 cm^{-1}	1.06
4% H_2	469 cm^{-1}	3.65	–	–	1165 cm^{-1}	0.66	1645 cm^{-1}	1.01
8% H_2	469 cm^{-1}	3.47	–	–	1154 cm^{-1}	1.08	1663 cm^{-1}	1.24

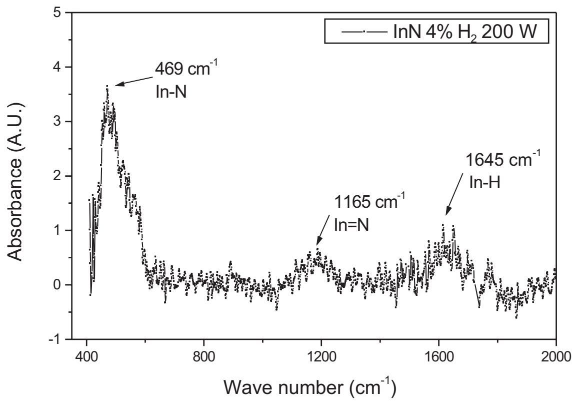

Figure 4 FT-IR peaks of the films produced with 4% hydrogen.

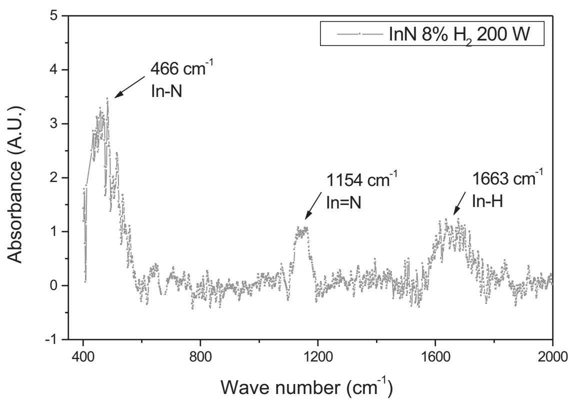

Figure 5 FT-IR peaks of the films produced with 8% hydrogen.

Table 5 RBS results for the films produced with 0, 2, and 4% hydrogen concentration.

sample	O (%)	N (%)	In (%)
0% H_2	8	65	27
2% H_2	–	65	35
4% H_2	–	55	45

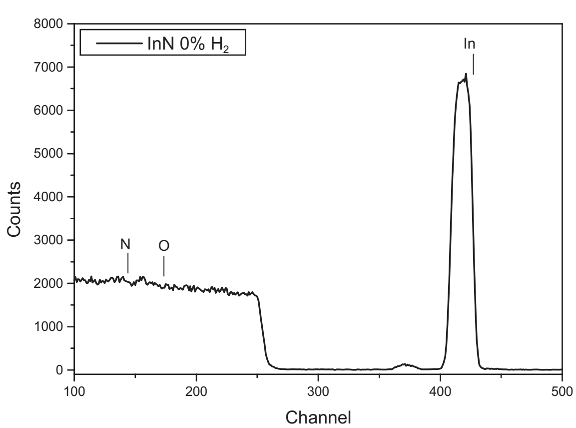

Figure 6 RBS spectra of the film produced without hydrogen.

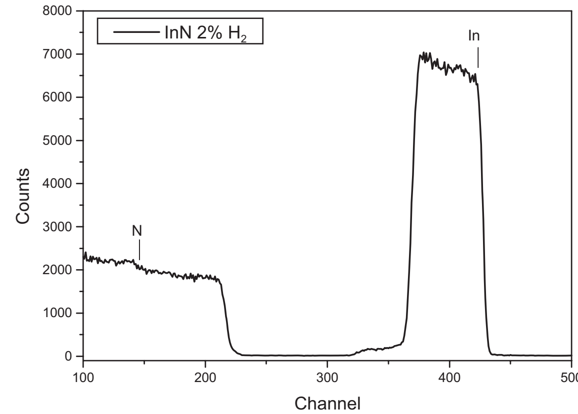

Figure 7 RBS spectra of the film produced with 2% hydrogen.

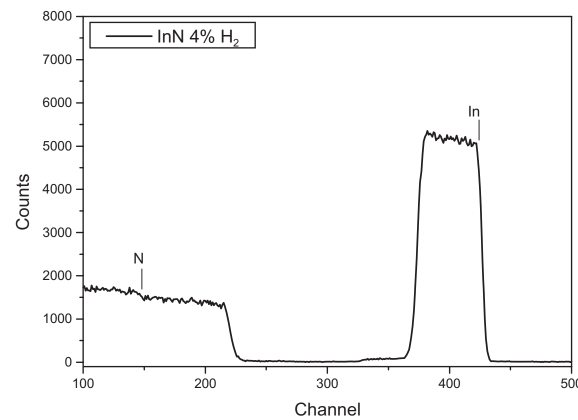

Figure 8 RBS spectra of the film produced with 4% hydrogen.

peak usually appears at 31.3°. The peak positions of the sputtered InN films appear at lower angles because the films present structural defects and impurities. XRD measurements presented InN (10$\bar{1}$0). This peak occurs for 2θ around 28°. At $2\theta \sim 33°$ a peak is observed known as an anomalous

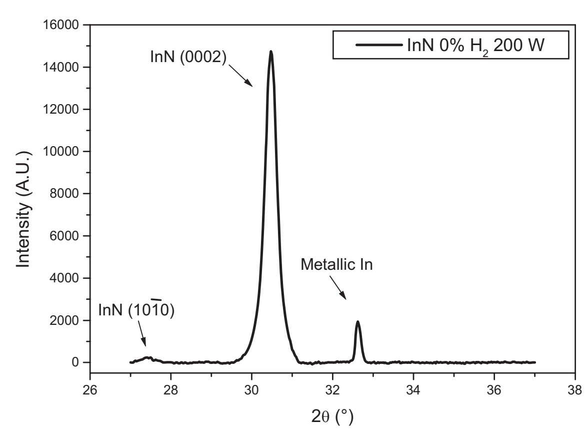

Figure 9 XRD diffractogram of the film produced without hydrogen.

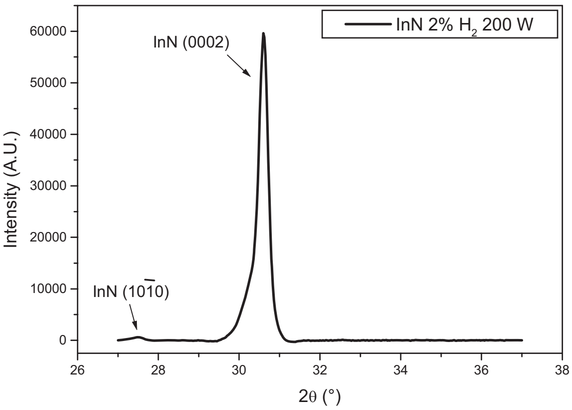

Figure 10 XRD diffractogram of the film produced with 2% hydrogen.

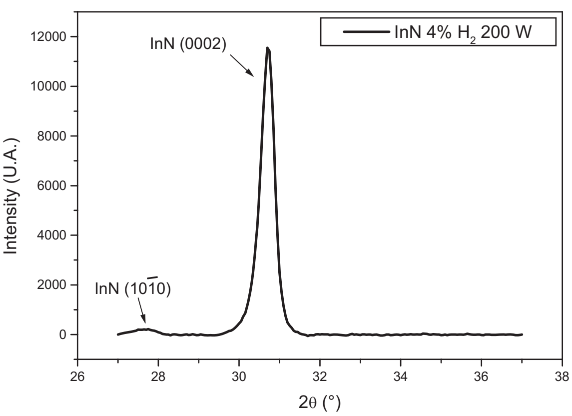

Figure 11 XRD diffractogram of the film produced with 4% hydrogen.

peak. It belongs to metallic indium and it occurs in InN pure samples.

Reflectance (%*R*) spectra were measured in the range 250–2500 nm in a Varian UV/Vis/NIR spectrophotometer

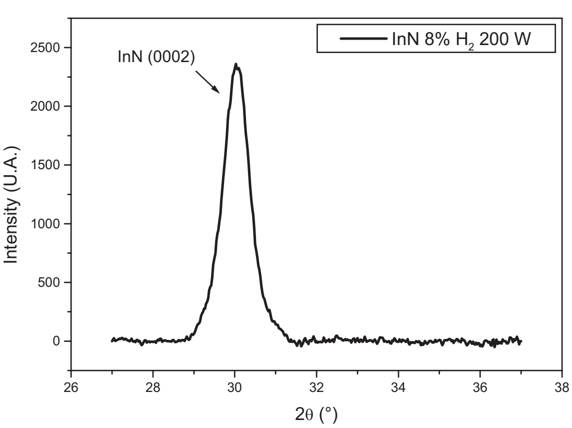

Figure 12 XRD diffractogram of the film produced with 8% hydrogen.

Table 6 X-ray diffraction results.

sample	peak 1 InN (10$\bar{1}$0)	peak 2 InN (0002)	peak 3 metallic In
0% H_2	27.65°	30.74°	32.64°
2% H_2	27.58°	30.71°	–
4% H_2	27.67°	30.76°	–
8% H_2	–	30.10°	–

for samples of InN thin film deposited on silicon substrate with different hydrogen gas concentrations (Fig. 13).

The bandgap was calculated for each sample from their reflectance spectra using Tauc analysis. The optical bandgap was estimated for samples deposited with 0, 2, 4, and 8% of hydrogen concentration in the gas mixture and the bandgap values obtained shown in Table 7.

It can be observed through these results that increasing the concentration of hydrogen causes an increase in the value of the bandgap. The bandgap of the films produced in this study are consistent with that expected for films deposited by sputtering. Usually, InN deposited by MBE and MOCVD have a bandgap much lower than that of a sputtered film (Fig. 14).

The pure InN has defects and metallic indium. Hydrogen eliminates the metallic indium and decreases the quantity of defects. This fact implies an increase of the bandgap.

In their study, Wu and Walukiewicz [15] report that as a result of the narrow gap of pure InN, this film has the lowest

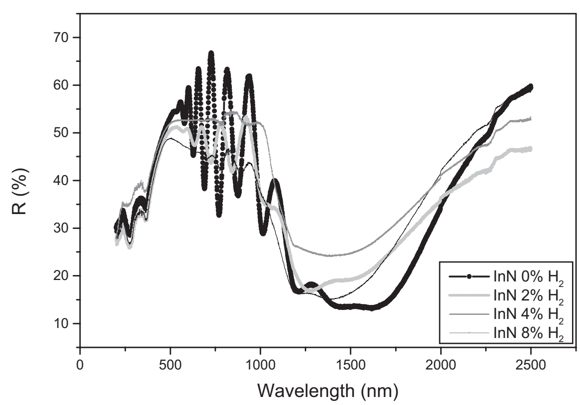

Figure 13 Reflectance spectra of samples deposited with 0, 2, 4, and 8% hydrogen.

Table 7 Bandgap.

sample	bandgap (eV)
0% H_2	1.31
2% H_2	1.49
4% H_2	1.98
8% H_2	2.33

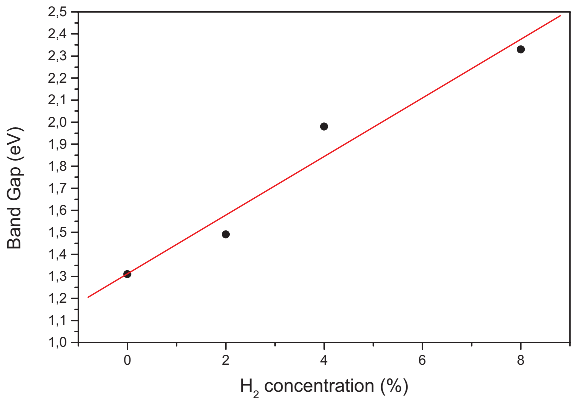

Figure 14 The optical bandgap was estimated for samples deposited with 0, 2, 4, and 8% of hydrogen concentration in the gas mixture.

conduction-band edge (next to the valence band) and thus the largest electron affinity of any semiconductor. Pure indium nitride is always n-type. When the hydrogen is incorporated, it modifies the InN to a p-type semiconductor, because it increases the distance between conduction and valence bands.

4 Conclusions Pure InN is naturally n-type and hydrogen eliminates some of the structural defects of this thin film. The hydrogen, when incorporated, amends for p-type semiconductor because it increases the distance between the valence and conduction bands. Examination of the infrared spectra reveals that there is In–H bonding. In fact, the hydrogen was incorporated in InN matrix and changed its electrical characteristics.

Acknowledgements The authors would like to thank to Dr. Luís da Silva Zambom, Mr. Alexandre Marques Camponucci, and Mr. Nelson Ordonez for technical support and FAPESP, CNPq and CAPES for financial support.

References

[1] W. Walukiewicz, P-type Indium Nitride Achieved, Berkeley Lab Research Highlight (2006).
[2] A. Janotti and C. G. Van de Walle, Appl. Phys. Lett. **92**, 032104 (2008).
[3] R. E. Jones, K. M. Yu, S. X. Li, W. Walukiewicz, J. W. Ager, E. E. Haller, H. Lu, and W. J. Schaff, Phys. Rev. Lett. **96**, 125505 (2006).
[4] M. Kumar, R. Chatterjee, S. Milikisiyants, A. Kanjilal, M. Voelskow, D. Grambole, K. V. Lakshmi, and J. P. Singh, Appl. Phys. Lett. **95**, 013102 (2009).
[5] M. Alevli, in: Growth and characterization of indium nitride layers grown by high pressure chemical vapor deposition, doctor thesis, 2008.
[6] M. Motlan, E. M. Goldys, T. L. Tansley, J. Cryst. Growth **241**, 165–170 (2002).
[7] S. Ruffenach, M. Moret, O. Briot, and B. Gil, Appl. Phys. Lett. **95**, 042102 (2009).
[8] E. A. Davis, S. F. J. Cox, and C. G. Valle, Appl. Phys. Lett. **82**, 592–594 (2003).
[9] S. Ruffenach, M. Moret, O. Briot, and B. Gil, Phys. Status Solidi A **207**, 9–18 (2010).
[10] V. Darakchieva, K. Lorenz, N. P. Barradas, E. Alves, B. Monemar, M. Schubert, N. Franco, C. L. Hsiao, L. C. Chen, W. J. Schaff, L. W. Tu, T. Yamaguchi, and Y. Nanishi, Appl. Phys. Lett. **96**, 081907 (2010).
[11] C. G. Valle, Physica B, 376–377 (2006).
[12] W. M. C. Hughes, M. L. Swanson, and J. C. Austin, J. Electron. Mater. **22**, 1011 (1993).
[13] W. Walukiewicz, J. W. Ager, III, K. M. Yu, Z. Liliental-Weber, J. Wu, S. X. Li, R. E. Jones, and J. D. Denlinger, Appl. Phys. **39**, 83–99 (2006).
[14] O. Takai, K. Ikuta, and Y. Inoue, Thin Solid Films **318**, 148–150 (1998).
[15] J. Wu and W. Walukiewicz, Superlattices Microstruct. **34**, 63 (2003).